

# Acrylamide/2-acrylamido-2-methylpropane sulfonic acid sodium salt-based hydrogels: synthesis and characterization

S. Durmaz<sup>a,b</sup>, O. Okay<sup>a,b,\*</sup>

<sup>a</sup>*Istanbul Technical University, Department of Chemistry, Maslak, 80626 Istanbul, Turkey*

<sup>b</sup>*TUBITAK Marmara Research Center, Department of Chemistry, Gebze, Kocaeli, Turkey*

Received 12 April 1999; received in revised form 7 July 1999; accepted 29 July 1999

## Abstract

Relationships between the formation mechanism and the swelling behavior of acrylamide (AAM)/2-acrylamido-2-methylpropane sulfonic acid sodium salt (AMPS)-based hydrogels were studied. The hydrogels were prepared by free-radical crosslinking copolymerization of AAM and AMPS at 40°C in the presence of *N,N'*-methylenebis(acrylamide) (BAAM) as the crosslinker. Both the crosslinker ratio (mole ratio of crosslinker to monomer) and the initial monomer concentration were fixed at 1/82 and 0.700 M, respectively, while the AMPS content in the monomer mixture was varied from 0 to 100 mol%. It was found that the copolymer composition is equal to the monomer feed composition, indicating that the monomer units distribute randomly along the network chains of the hydrogels. The monomer conversion versus time histories as well as the growth rate of the gel during the polymerization were found to be independent of the amount of AMPS in the initial monomer mixture. It was shown that the reaction system separates into two phases at the gel point and the gel grows in a heterogeneous system. The equilibrium degree of swelling of the final hydrogels increases with increasing AMPS content until a plateau is reached at about 10 mol% AMPS. Between 10 and 30 mol% AMPS, the equilibrium gel swelling in water as well as in aqueous NaCl solutions was independent on the ionic group content of the hydrogels. Further increase in the AMPS content beyond this value increased the gel swelling continuously up to 100 mol%. The polyelectrolyte theories based on the counterion condensation cannot explain the observed swelling behavior of AAM/AMPS hydrogels. The swelling curves of the hydrogels in water and in aqueous NaCl solutions were successfully reproduced with the Flory–Rehner theory of swelling equilibrium including the ideal Donnan equilibria, where the effective charge density was taken as an adjustable parameter. Scaling rules were derived for the ionic group content and the effective excluded volume of the hydrogels. © 2000 Elsevier Science Ltd. All rights reserved.

**Keywords:** Acrylamide; 2-acrylamido-2-methylpropane sulfonic acid sodium salt; Hydrogel formation

## 1. Introduction

In recent years, hydrogels derived from acrylamide (AAM) have received considerable attention for use as specific sorbents and as support carriers in biomedical engineering. AAM-based hydrogels are prepared mainly by free-radical crosslinking copolymerization of the AAM monomer with the *N,N'*-methylenebis(acrylamide) (BAAM) crosslinker. In order to increase their swelling capacity, an ionic comonomer is also included in the monomer mixture. The swelling behavior of polymer gels is known to depend on their network structure whereas the latter is closely related to the conditions under which the polymer gels are formed. Thus, the understanding of the formation

mechanism of hydrogels is of great interest in predicting their physical properties.

Although extensive work has been reported in the literature for the swelling and collapse phenomena in AAM-based hydrogels [1,2], only a few were concerned with their formation mechanism [3–6]. The aim of this work was to investigate the formation process of AAM-based hydrogels by free-radical crosslinking copolymerization. For this investigation, we selected 2-acrylamido-2-methylpropane sulfonic acid sodium salt (AMPS) as the ionic comonomer of AAM. AMPS has received attention in the last few years due to its strongly ionizable sulfonate group; AMPS dissociates completely in the overall pH range, and therefore, the hydrogels derived from AMPS exhibit pH independent swelling behavior. It was shown that the linear polymers with sulfonate groups derived from AMPS exhibit extensive coil expansion in aqueous solutions; even in a 5 M NaCl solution, the expansion of polymer coils due to charge repulsion cannot be totally screened [7]. Liu et al. investigated

\*Corresponding author. Istanbul Technical University, Department of Chemistry, Maslak, 80626 Istanbul, Turkey. Fax: +90-0262-6412300.

E-mail address: oguz@mam.gov.tr (O. Okay).

the swelling properties of hydrogels derived from AMPS and *N,N*-dimethylacrylamide (DMAA) and observed a similar behavior [8]. Tong and Liu observed a constant swelling capacity of AMPS/DMAA hydrogels in the whole pH range and concluded that the AMPS content of the hydrogel corresponds to its charge density [9]. Their calculation results showed a large discrepancy between the measured swelling data in water and that predicted by the Flory–Rehner theory of swelling equilibrium [9]. We investigated the swelling behavior of AAm/AMPS hydrogels in water and in aqueous salt solution. In contrast to Tong and Liu, we observed a good agreement between the Flory–Rehner theory and experiment [10].

All the studies mentioned above only dealt with the physical properties of the final hydrogels without considering their formation history. The present work focuses on the relationships between the formation mechanism and the swelling behavior of AAm/AMPS hydrogels. In this study, a series of hydrogels was prepared in the presence of BAAM as the crosslinker such that the crosslinker ratio (mole ratio of crosslinker to monomer) and the initial monomer concentration were fixed, while the AMPS content in the monomer mixture was varied from 0 to 100 mol%. We have investigated the comonomer reactivities, time-conversion profiles, the growth rate and the swelling properties of the hydrogels depending on the initial monomer composition.

## 2. Experimental

### 2.1. Materials

Acrylamide (AAm, Merck) was crystallized from acetone/ethanol mixture (70/30 by volume) below 30°C. 2-acrylamido-2-methylpropane sulfonic acid (AMPS-H<sup>+</sup>, Merck) was crystallized from boiling methanol. The purity of the monomers was checked by i.r., n.m.r. and elemental microanalysis. 2-acrylamido-2-methylpropane sulfonic acid sodium salt (AMPS) stock solution was prepared by dissolving 20 g of AMPS-H<sup>+</sup> in about 40 ml of distilled water and adding to this solution 10 ml of a 30% NaOH solution under cooling. Then, the solution was titrated with 1 M NaOH to pH = 7.00 and finally, the volume of the solution was completed to 100 ml with distilled water. AMPS stock solution (1 ml) of thus prepared contained 0.966 mmol AMPS. *N,N'*-methylenebis(acrylamide) (BAAM, Merck) and potassium persulfate (KPS, Merck) were used as received. KPS stock solution was prepared by dissolving 0.040 g of KPS in 10 ml of distilled water. Distilled and deionized water was used for the swelling experiments. For the preparation of the stock solutions and for the hydrogel synthesis, distilled and deionized water was distilled again prior to use and cooled under nitrogen bubbling.

### 2.2. Synthesis of hydrogels

AAm/AMPS crosslinking copolymerization was carried

out in water, as the polymerization solvent, at 40°C in the presence of 0.474 mM with KPS as the initiator. Both the crosslinker ratio (mole ratio of the crosslinker BAAM to the monomers AAm + AMPS) and the total monomer concentration were fixed at 1/82 and 0.700 M, respectively, whereas the AMPS content of the monomer mixture was varied from 0 to 100 mol%. To illustrate the synthetic procedure, we give details for the preparation of the hydrogel with 40 mol% AMPS in the comonomer feed composition:

AAm (2.982 g), AMPS stock solution (29.0 ml), BAAM (0.1314 g), and KPS stock solution (3.2 ml) were dissolved in 67.8 ml of distilled water. After bubbling nitrogen for 20 min, the solution was poured into several glass tubes of 11 or 5.5 mm internal diameters and about 250 mm long. Thereafter, 10 min of nitrogen bubbling was required through each solution to obtain reproducible results. The glass tubes were sealed, immersed in a thermostated water bath at 40°C and the polymerization was conducted for predetermined reaction times. Temperature measurements showed a temperature rise inside the reaction solution less than 1°C, indicating that the dilute reaction condition provides a nearly isothermal condition. Homologous series of hydrogels were prepared in this way allowing systematic variation of the reaction time and the AMPS content of the monomer mixture. We observed that the diameter of the gel samples (11 or 5.5 mm) does not affect the polymerization kinetics as well as the properties of the resulting hydrogels.

### 2.3. Gel points

Gel point measurements were carried out using two different methods. First, the gravimetric technique was used to follow the gelation process. The gel point was determined as the midpoint between the last time at which a soluble polymer was obtained and that at which the polymer was not soluble in water. For ascertaining the insoluble gel component of the samples, the latter were treated with an approximately 50-fold excess of water at room temperature. The formation of insoluble polymers was detected visually from the appearance of gel particles in water. Second, dilatometers containing a teflon-covered steel sphere of 5 mm diameter was used for the gel point measurements. The midpoint between the last time at which the sphere moves magnetically and that at which it stops moving is taken as the gel point [5].

### 2.4. Gel fraction

Water was chosen as the extraction solvent for the crude hydrogels and employed at room temperature. After the predetermined polymerization times, the reaction was stopped by cooling the reaction mixture in an ice-water bath. The crude hydrogels, 11 or 5.5 mm in diameter, were freed from the glass tubes and they were cut into samples of about 10 mm length. Each sample was placed in an excess of water containing a small amount of

hydroquinone as an inhibitor, and the solvent was replaced every other day over a period of at least one week until no further extractable polymer could be detected. The hydrogels after extraction were carefully deswollen in a series of water–acetone mixtures with increasing acetone content. This solvent exchange process facilitated final drying of the hydrogel samples. They were then washed several times with acetone and dried at 70°C under vacuum to constant weight. The amount of soluble polymer in water solution was determined gravimetrically after evaporation and precipitation in acetone. The weight fraction of gel  $W_g$  was calculated as

$$W_g = \frac{m_{\text{gel}}}{m_{\text{gel}} + m_{\text{sol}}} \quad (1)$$

where  $m_{\text{gel}}$  and  $m_{\text{sol}}$  are the weights of extracted dry hydrogel and of the soluble polymer, respectively.

### 2.5. Swelling measurements in water

After the predetermined polymerization times, the hydrogels in glass tubes of 11 or 5.5 mm in diameter, were freed from the tubes and they were cut into samples of about 10 mm length. The initial diameter of the gel samples,  $D_0$ , was measured by a calibrated digital compass. Then, each sample was placed in an excess of water at room temperature ( $19 \pm 1^\circ\text{C}$ ). In order to reach the equilibrium degree of swelling, the hydrogels were immersed in water for at least two weeks during which water was replaced every other day; the swelling equilibrium was tested by weighing the samples, or by measuring their diameters. To achieve good precision, three measurements were carried out on samples of different length taken from the same gel.

For the measurement of the equilibrium weight swelling ratio,  $q_w$ , the hydrogels were weighed in the swollen state and dried, after a solvent exchange with acetone as described above, under vacuum to constant weight. The equilibrium weight swelling ratio  $q_w$  was calculated as

$$q_w = \frac{m_s}{m_d} \quad (2)$$

where  $m_s$  and  $m_d$  are the weights of the hydrogels in the swollen state and the dry state, respectively.

The equilibrium volume swelling ratio of the complete-conversion hydrogels  $q_v$  (volume of swollen gel/volume of dry gel) was determined by measuring the diameter of the hydrogel samples by a calibrated digital compass.  $q_v$  was calculated as

$$q_v = \left( \frac{\text{volume of the equilibrium swollen gel}}{\text{volume of the gel after synthesis}} \right) \times \left( \frac{\text{volume of the gel after synthesis}}{\text{volume of dry gel}} \right) \quad (3a)$$

$$q_v = \left( \frac{D}{D_0} \right)^3 \left( \frac{1}{v^0} \right) \quad (3b)$$

where  $D$  and  $D_0$  are the diameters of the hydrogels after equilibrium swelling in water and after synthesis, respectively, and  $v^0$  is the volume fraction of the network after synthesis. Note that if one starts with a dry gel, since  $v^0 = 1$ , Eq. (3b) reduces to  $q_v = (D/D_0)^3$ . However, in the present work, as the hydrogels form in a solution, this already corresponds to a certain degree of swelling after gel synthesis, which is represented by  $(v^0)^{-1}$  in Eq. (3b). Thus,  $(v^0)^{-1}$  represents the volume degree of swelling of the hydrogels after their synthesis. The  $v^0$  of complete-conversion hydrogels was calculated from the mole fraction of the AMPS units in the network  $F_2$  and the molecular weights of AMPS and AAm (229 and 71 g/mol, respectively) as:

$$v^0 = 0.700 \times 10^{-3} [229F_2 + 71(1 - F_2)]/\rho \quad (4)$$

where  $\rho$  is the density of the polymer. The literature values of  $\rho$  for the poly(acrylamide) network and for poly(2-acrylamido-2-methylpropanesulfonamide) derived from poly(AMPS- $\text{H}^+$ ) are 1.35 and 1.443 g/cm<sup>3</sup>, respectively [11,12]. For the calculations, we assumed a constant density of 1.35 g/cm<sup>3</sup> for all the hydrogels.

### 2.6. Swelling measurements in salt solutions

The swelling measurements were carried out in aqueous NaCl solutions at room temperature. The concentration of NaCl solutions ranged from  $10^{-5}$  to 1.0 M. The hydrogels equilibrium swollen in water were transferred to vials containing the most diluted aqueous NaCl solution. The gel samples were allowed to swell in the solution for two weeks, during which aqueous NaCl was refreshed to keep the concentration as needed. After the swelling equilibrium is established, swelling measurements were carried out as described in the previous section. The gel samples were then transferred into the next concentrated NaCl solution. The swelling measurements in aqueous NaCl were carried out both in the direction of increasing salt concentration and in the reverse direction. No systematic variation in the recorded swelling data was observed.

### 2.7. Hydrogel composition

In order to determine the chemical composition of the hydrogels, a series of AAm/AMPS copolymers was prepared under the same reaction condition as the hydrogels except that the BAAm crosslinker was not used. The copolymerization reactions were stopped at fractional monomer conversions  $x$  less than 0.20. The reaction solution was diluted with water and then poured in an excess of acetone. The precipitated copolymer was dried at room temperature until constant weight.

Two independent techniques were used to determine the composition of AAm/AMPS copolymers. First, the AMPS content of dried copolymers was estimated from i.r. spectra. The i.r. spectra of the samples in KBr pellets were recorded on a Perkin–Elmer 983 spectrophotometer. A typical

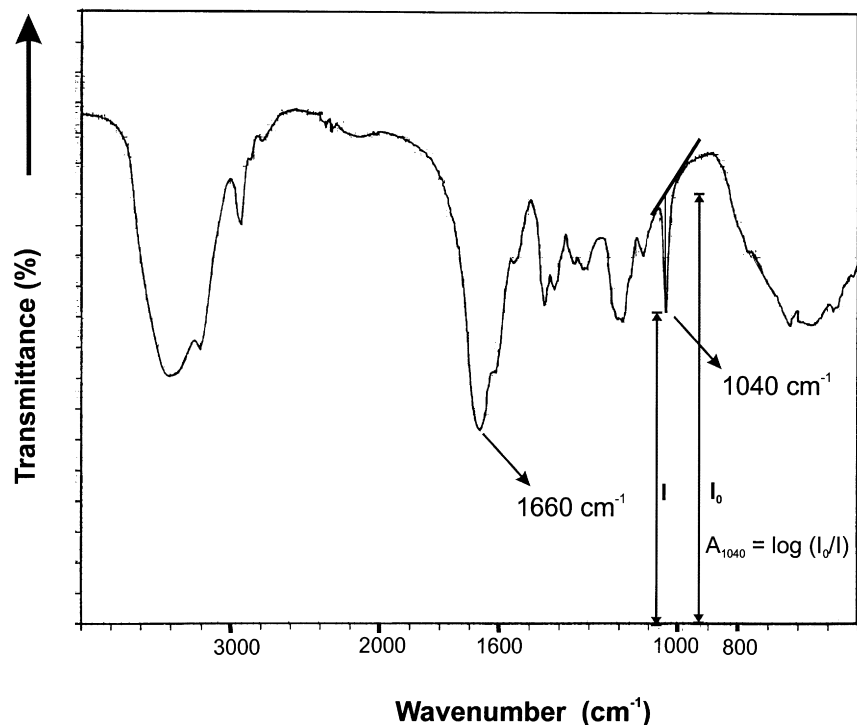


Fig. 1. IR spectrum of an AAm/AMPS network with 10 mol% AMPS in the KBr pellet. The calculation of absorbance is shown schematically at  $1040\text{ cm}^{-1}$ .

spectrum of AAm/AMPS copolymers is shown in Fig. 1. The characteristic absorption peak of AMPS units is shown at  $1040\text{ cm}^{-1}$  due to the SO group. The intensity of this peak was normalized using the C=O stretching peak of both AAm and AMPS units at  $1660\text{ cm}^{-1}$ . The calculation of the

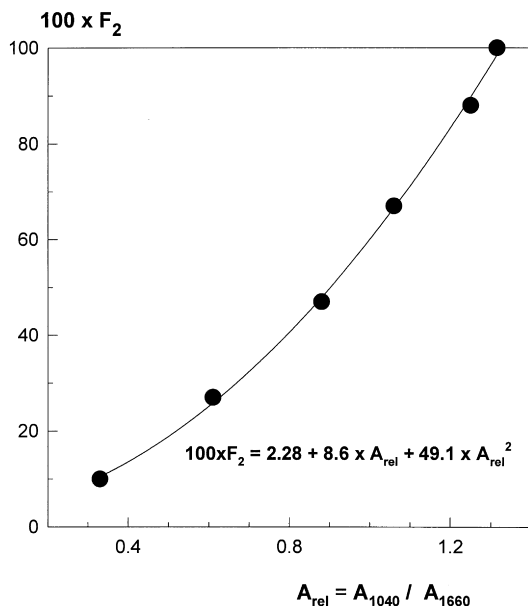


Fig. 2. The calibration curve showing the AMPS mole fraction in the AAm/AMPS copolymer  $F_2$  as a function of the ratio of absorbances  $A$  at  $1040$  to  $1660\text{ cm}^{-1}$ .

absorbances at  $1040$  and  $1660\text{ cm}^{-1}$  ( $A_{1040}$  and  $A_{1660}$ , respectively) was performed using the base-line method [13] (Fig. 1). In order to quantify the results, a calibration curve was prepared using polymer samples prepared by mixing linear poly(AAm) and poly(AMPS) homopolymers in the predetermined mole ratio. The calibration curve showing the AMPS mole fraction in the copolymer  $F_2$  as a function of the  $A_{1040}/A_{1660}$  ratio is given in Fig. 2.

Secondly, elemental microanalysis results of the copolymer samples were used to estimate their chemical composition. The C, H, and N analysis were performed on a Carlo Erba 1106 elemental analyzer, while the S content was determined by the Leco SC 32 sulfur analyzer (ASTM 4239-93). The interpretation of the microanalysis results was however complicated due to the bounded water in the polymer samples. It was found that the homopolymers or copolymers of AAm and AMPS always contained about 10 wt% water, even after several months of drying at room temperature under vacuum. Therefore, two unknowns existed for each copolymer sample, namely their AMPS and water contents. Let  $w$  be the weight fraction of water in the dried copolymer, C, N, and S contents can be calculated using the equations:

$$C\% = \frac{12((3/F_2) + 4)}{\bar{M}_r} \times 100 \quad (5a)$$

$$N\% = \frac{14/F_2}{\bar{M}_r} \times 100 \quad (5b)$$

Table 1

Elemental microanalysis results of AAm/AMPS copolymers.  $f_2$  is the mole fraction of AMPS in the initial comonomer mixture;  $F_2$ , the mole fraction of AMPS in the copolymer chains;  $w$ , the weight fraction of water in the dried copolymers;  $F_2$  and  $w$  were calculated by fitting Eqs. (5a)–(5d) to the observed C, N, S contents

$10^2 f_2$	$10^2 F_2$	$W$	C%		H%		N%		S%	
			Found	Calculated	Found	Calculated	Found	Calculated	Found	Calculated
0	0	$0.13 \pm 0.01$	44.7	44.1	6.6	7.6	17.0	17.2	–	–
10	$9.7 \pm 0.8$	$0.12 \pm 0.01$	41.5	41.2	7.2	7.1	14.1	14.2	3.0	3.1
20	$18 \pm 2$	$0.10 \pm 0.02$	41.1	40.5	6.8	6.8	12.5	12.7	4.9	5.2
30	$29 \pm 2$	$0.14 \pm 0.02$	37.4	36.9	6.3	6.7	10.2	10.4	6.5	6.8
40	$36 \pm 8$	$0.09 \pm 0.06$	39.8	38.0	6.5	6.4	9.3	10.0	7.3	8.1
50	$50 \pm 10$	$0.13 \pm 0.05$	36.4	34.8	5.4	6.4	7.5	8.1	8.4	9.2
60	$55 \pm 15$	$0.14 \pm 0.07$	36.6	34.0	5.6	6.4	6.6	7.6	8.5	9.6
70	$64 \pm 22$	$0.10 \pm 0.10$	38.8	34.7	6.7	6.1	5.7	7.3	9.1	10.6

$$S\% = \frac{32}{\bar{M}_r} \times 100 \quad (5c)$$

where  $\bar{M}_r$  is the molecular weight of the repeat unit (AAm + AMPS + bounded water), i.e.

$$\bar{M}_r = (158 + 71/F_2)/(1 - w) \quad (5d)$$

Fitting Eqs. (5a)–(5d) to the observed elemental microanalysis data allowed calculations of the two unknowns  $F_2$  and  $w$ .

### 3. Results and discussion

#### 3.1. AAm/AMPS reactivities

The composition of the network chains in the hydrogels

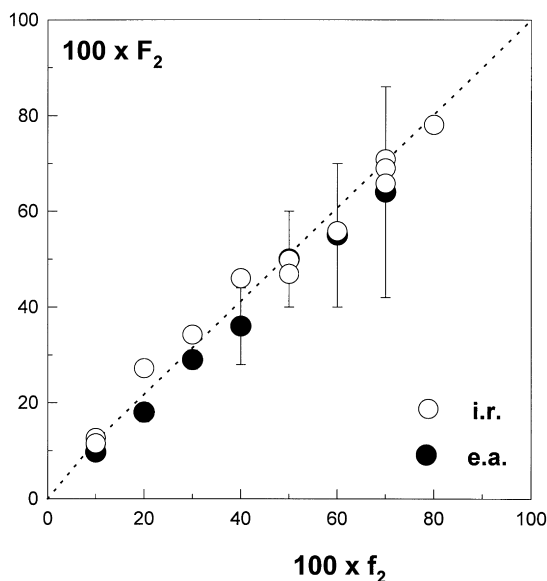


Fig. 3. The AMPS mole fraction in the network  $F_2$  evaluated by i.r. (open symbols) and by e.m. techniques (filled symbols) shown as a function of the AMPS mole fraction in the feed  $f_2$ . The dotted line represents the relation  $F_2 = f_2$ .

was estimated by i.r. and by elemental microanalysis (e.m.) techniques, as described in the previous section. By the i.r. technique, the ratio of the absorbances of the copolymers at 1040 to 1660  $\text{cm}^{-1}$  together with the calibration curve shown in Fig. 2 allowed calculation of the AMPS mole fraction  $F_2$  in the copolymers. By the e.m. technique, Eqs. (5a)–(5c) were fitted to the observed chemical composition of dried copolymers giving  $F_2$  and the water content  $w$  of the samples. Table 1 shows the measured elemental composition of some dried AAm/AMPS copolymers together with the fit results. The standard deviations in the calculations of  $F_2$  and  $w$  are also shown in the table. It is seen that the AAm/AMPS copolymers after constant weight drying at room temperature still contain water with about 10 wt%. For AMPS mole fractions in the feed  $f_2 < 0.40$ , calculation results provide good agreement with the observed values and the standard deviations in  $F_2$  and  $w$  are small. However, discrepancies between the observed and calculated values appear as  $f_2$  further increases and the standard deviations become larger.

In Fig. 3, the AMPS mole fraction in the copolymer  $F_2$  evaluated by i.r. (open symbols) and e.m. techniques (filled symbols) is shown as a function of the AMPS mole fraction in the feed  $f_2$ . The dotted straight line represents the relation  $F_2 = f_2$ . It is seen that the straight line gives a good fit with the data, indicating that the copolymer composition is almost equal to the monomer feed composition. This suggests that the monomer units distribute randomly along the network chains of the hydrogels, i.e. both the reactivity ratios  $r_1$  and  $r_2$  in AAm/AMPS copolymerization are close to unity ( $r_1 = r_2 \cong 1$ ).

#### 3.2. Hydrogel formation

Fractional monomer conversion  $x$  versus time  $t$  histories in AAm/AMPS crosslinking copolymerization are shown in Fig. 4 for various monomer feed compositions. The reaction temperature was 40°C and the total monomer and the initiator concentrations were 0.700 M and 0.474 mM, respectively. All the experiments were for a fixed crosslinker

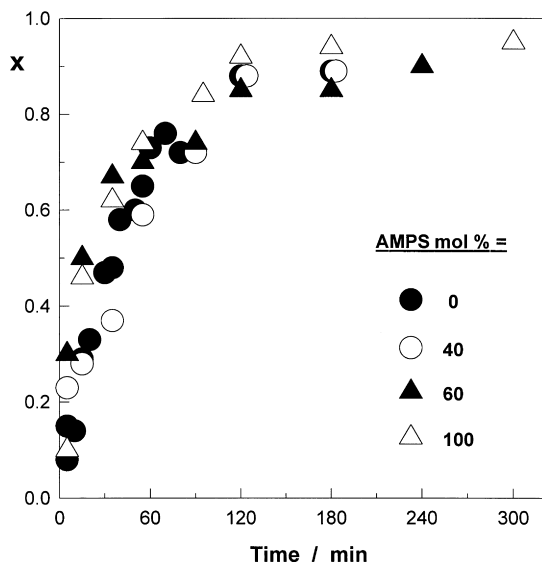


Fig. 4. Fractional monomer conversion  $x$  versus time histories in AAm/AMPS crosslinking copolymerization at 40°C. The data points for 0 mol% AMPS were taken from Ref. [14].

ratio of 1/82. The data points for the crosslinking polymerization of AAm without AMPS were taken from the literature [14]. Each data point in Fig. 4 is an average of four to seven separate experiments; standard deviations are smaller than the symbols themselves. According to Fig. 4, the monomer feed composition does not affect the rate of polymerization. This is expected from the results of the previous section. The monomer conversion  $x$  increases with the reaction time up to 2 h; for longer reaction times up to 5 h,  $x$  remained almost constant at a limiting value of 0.9.

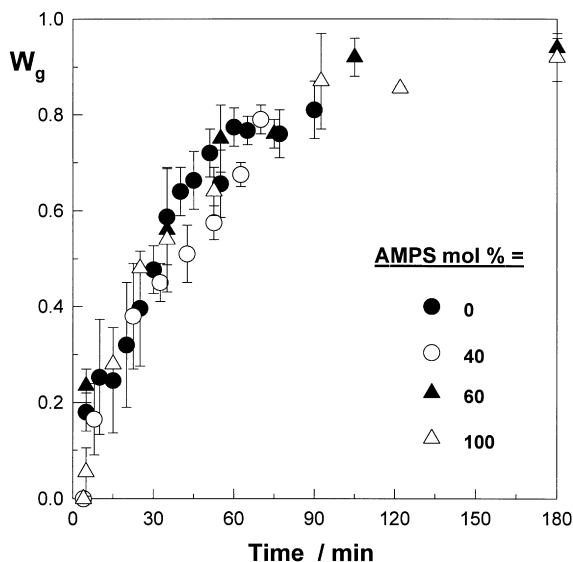


Fig. 5. The weight fraction of gel,  $W_g$ , shown as a function of the reaction time in AAm/AMPS crosslinking copolymerization. The error bars indicate the standard deviations. The data points for 0 mol% AMPS were taken from Ref. [14].

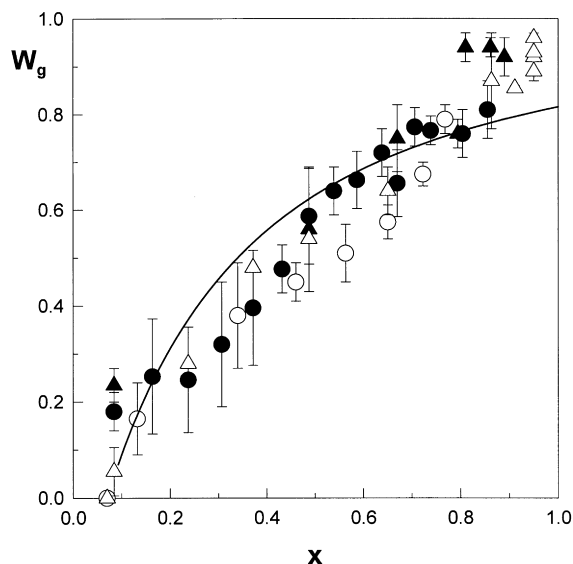


Fig. 6. The weight fraction of gel,  $W_g$ , shown as a function of the fractional monomer conversion  $x$  in AAm/AMPS crosslinking copolymerization. The error bars indicate the standard deviations. The solid curve is the best fitting curve of Eqs. (6) and (7) to the experimental data for  $n = 2$ . The data points for 0 mol% AMPS were taken from Ref. [14]. See Fig. 5 for symbol keys.

The first insoluble polymer in the reaction mixture appeared after a reaction time  $t_c = 4 \pm 1$  min or, after a monomer conversion  $x_c = 0.07 \pm 0.02$ . This critical point was found to be independent of the monomer feed composition. However, by use of the dilatometric technique, we observed that at this point the microsphere inside the dilatometer stopped moving only in the lower part of the solution. Repeated measurements indicated formation of gel regions distributed inside a solution phase. Thus, instead of gelling of the overall reaction system at  $t_c$  (or at  $x_c$ ), gel particles started to appear in the reaction system. This phenomena was observed for all monomer feed compositions studied. This means that the volume of the first formed gel is not equal to the reaction volume so that the reaction mixture separates into two phases at the critical time for the onset of a macroscopic network: a swollen gel phase and the solution phase [14]. Because the refractive indices of both phases do not differ from each other, the reaction mixture remained transparent during the polymerization. As the polymerization and crosslinking reactions proceed, the heterogeneous reaction system turned again into a homogeneous one.

In Figs. 5 and 6, the weight fraction of gel  $W_g$  is shown as a function of the reaction time  $t$  and the monomer conversion  $x$ , respectively.  $W_g$  rapidly increases with increasing reaction time or monomer conversion and reaches a limiting value of 0.92 after about 2 h (Fig. 5). Within the limits of experimental error, the growth rate of the gel is independent of the comonomer feed composition. According to the statistical theory of gelation [15], the gel fraction depends on the crosslink density of the overall reaction system  $\bar{\rho}$  and on the chain length distribution of the primary molecules,

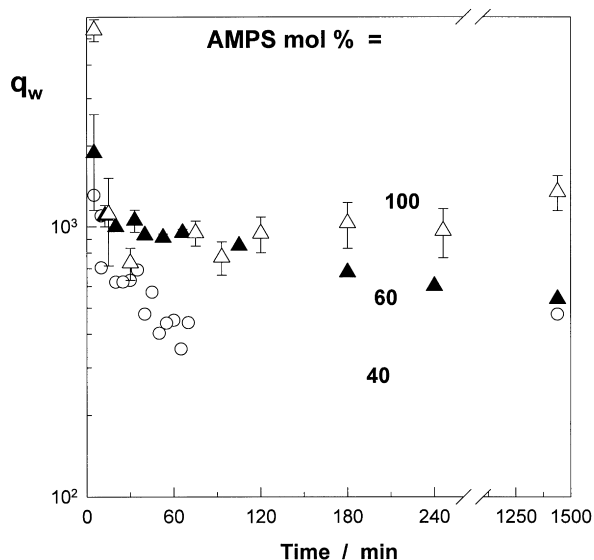


Fig. 7. The equilibrium weight swelling ratio  $q_w$  of the hydrogels isolated at various reaction times shown as a function of the reaction time in AAm/AMPS crosslinking copolymerization. The error bars indicate the standard deviations.

i.e.

$$W_s = \sum_{r=1}^{\infty} w_r [1 - \bar{\rho}(1 - W_s)]^r \quad (6)$$

where  $W_s$  is the weight fraction of sol ( $1 - W_g$ ),  $w_r$  is the weight fraction of primary molecules composed of  $r$  units. Substitution of certain molecular weight distributions of

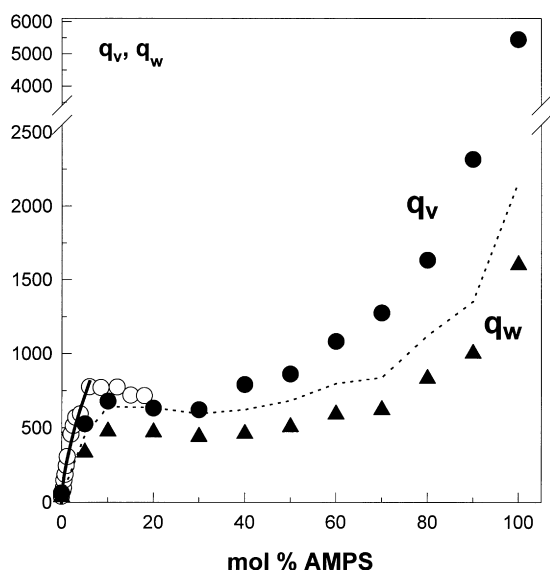


Fig. 8. The equilibrium volume  $q_v$ , and the equilibrium weight swelling ratio  $q_w$  of the hydrogels shown as a function of their AMPS contents. The open circles are the  $q_v$  values of the AAm/AMPS-based hydrogels taken from Ref. [10]. The solid curve is the best fitting curve for 0 to 8 mol% AMPS,  $q_v \propto (\text{AMPS mol}\%)^{0.63}$ . The dotted curve represents the calculated  $q_v$  values using Eq. (8) from the experimental  $q_w$  values.

primary molecules into Eq. (6) yields [16]:

$$\sum_{i=1}^n W_s^{i/n} = \frac{n}{\varepsilon} \quad (n = 2 \text{ and } 3) \quad (6a)$$

where  $\varepsilon$  is the number of crosslinked units per weight-average primary molecule,  $n = 2$  for Flory's most probable molecular weight distribution, and  $n = 3$  for primary molecules formed by radical combination. One of the assumptions used in the derivation of Eq. (6) is the random formation of crosslinks between the polymer molecules. This assumption is equivalent to stating that  $\varepsilon$  is a linear function of  $x$ , i.e.

$$\varepsilon = 1 + a(x - x_c) \quad (7)$$

where  $a$  is a constant. The best fitting curve of Eqs. (6) and (7) for  $n = 2$  to the experimental  $W_g$  versus  $x$  data data gives the solid curve in Fig. 6 with  $a = 2.44$ . It is seen that the theory predicts a much steeper rise in the amount of gel than the observed results for  $x < 0.40$ . Then, in the region of higher monomer conversions, the gel fraction curve given by the statistical theory gradually bends downward apart from the observed tendency. Calculation results for  $n = 3$  also gave a similar curve. We may conclude that the statistical theory only qualitatively predicts the gel growth in the reaction system. The deviation between the theory and experiments can be attributed to the nonuniform distribution of crosslinks in the hydrogels [17] and/or to the gel effect and the resulting acceleration in the growth rate of the gel [18]. These two features of the gel formation processes were not taken into account in the derivation of Eq. (6). The growing gel isolated at various reaction times was immersed in an excess of water and its equilibrium weight swelling ratio  $q_w$  was measured. Fig. 7 illustrates how  $q_w$  varies with the reaction time for various monomer feed compositions. The equilibrium swelling ratio  $q_w$  decreases abruptly in the first 60 min of the reaction time, and then  $q_w$  begins to approach an equilibrium value.

### 3.3. Hydrogel swelling

AAm/AMPS hydrogels of various compositions were prepared under the same reaction condition as above but, the reaction time was set to 24 h. Both the gel fraction and the monomer conversion were found to be larger than 0.98. This means that the limiting conversion (0.9) and the limiting gel fraction (0.92) values observed between 2 and 5 h further increased by prolonged reaction times. After extraction of the hydrogels with water, their equilibrium swelling ratios in water and in aqueous NaCl solutions of concentrations ranged from  $10^{-5}$  to 1 M were measured by both gravimetric and volumetric techniques.

Fig. 8 shows how the equilibrium volume ( $q_v$ ) and the equilibrium weight swelling ratios ( $q_w$ ) of the hydrogels vary with their AMPS content. In Fig. 9,  $q_v$  values of the hydrogels are plotted as a function of the salt concentration in the external solution. Each data point in Figs. 8 and 9 is an

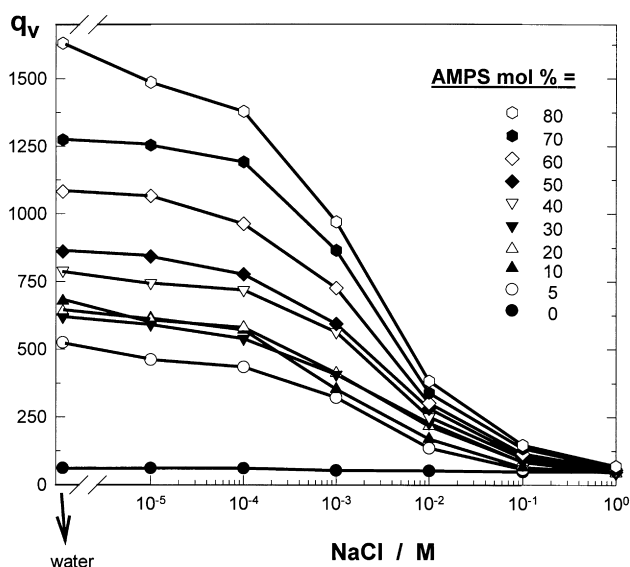


Fig. 9. The equilibrium volume swelling ratio  $q_v$  of the hydrogels shown as a function of the NaCl concentration in the external solution. The solid curves only show the trend of the data.

average of three separate experiments. The standard deviations (not shown in the figures) were less than 10%. The open symbols in Fig. 8 represent  $q_v$  values of the hydrogels taken from Ref. [10]. Note that there is an interrelation between  $q_v$  and  $q_w$  values [19]. Assuming additivity of volumes within the swollen gel, this relation is given by:

$$q_v = 1 + \frac{(q_w - 1)\rho}{d_1} \quad (8)$$

where  $d_1$  is the density of water ( $1 \text{ g/cm}^3$ ). The dotted curve in Fig. 8 illustrates the calculated  $q_v$  values using Eq. (8). It can be seen that the calculated  $q_v$  is in agreement with its experimental value for  $<40\%$  AMPS contents, whereas they differ at higher AMPS contents. This may be due to the bounded water in the hydrogels after drying which results in smaller experimental  $q_w$  and calculated  $q_v$  values.

Fig. 8 illustrates that, contrary to the classical theory of swelling equilibrium [15], the equilibrium degree of swelling is not a monotonically increasing function of the ionic group content of the hydrogels. The dependence of the gel swelling on the charge density shows three stages. First, the degree of swelling increases sharply with increasing ionic group content of the hydrogels until a plateau is reached at about 10 mol% AMPS. Secondly, between 10 and 30 mol% AMPS, the equilibrium gel swelling in water (Fig. 8) as well as in aqueous NaCl solutions (Fig. 9) is independent of the ionic group content of the hydrogels. Thirdly, further increase in the AMPS content beyond this value increases the gel swelling continuously up to 100 mol%.

Increasing degree of equilibrium swelling with increasing ionic group content of the hydrogels or, with decreasing salt concentration in the external solution is expected. This is a consequence of the osmotic pressure exerted by counterions of the AMPS units in the network chains. This osmotic

pressure increases as the concentration difference of the counterions between the inside and outside the gel phase increases. Thus, the swelling behavior of the hydrogels prepared at low and high concentration of AMPS is expected.  $q_v$  versus AMPS content dependence below the plateau region gives a scaling relation  $q_v \propto (\text{AMPS mol}\%)^{0.63}$ , shown in Fig. 8 by the solid curve. This stands in contrast to that predicted by the Flory–Rehner theory, if applied to highly swollen hydrogels [15],  $q_v \propto (\text{AMPS mol}\%)^{1.5}$ .<sup>1</sup> Recent experimental results obtained with poly(acrylic acid) (PAAc) hydrogels [20] as well as with AMPS/DMAA-based hydrogels [21] gave a scaling parameter 0.6, which is close to the value found in this work. We believe that the deviation between the theory and experiment originates from the existence of “wasted” counterions in the hydrogels. This point is discussed later on.

As seen in Fig. 8, the hydrogels prepared between 10 and 30 mol% AMPS exhibit the same degree of swelling. In weak electrolyte hydrogels, the appearance of a plateau region in the swelling curve was observed previously. Silberberg et al. reported that the equilibrium swelling degree of PAAc hydrogels first increases when the ionization degree  $\alpha$  of AAc units increases from 0 to 0.35; then, the gel swelling reaches a plateau up to  $\alpha = 1$  [20]. For the same hydrogels, Tong and Liu reported that the gel swelling is independent of  $\alpha$  between  $\alpha = 0.2$  and 0.6 [22]. Konak and Bansil observed a broad minimum in the swelling curve of poly(methacrylic acid) hydrogels between  $\alpha = 0.1$  and 0.2, whereas the degree of swelling begins to decrease for  $\alpha > 0.2$  [23]. This feature of the hydrogels may be related to the “counterion condensation” or to the limited extensibility of the network chains [24].

Following Manning’s theory [25], if the distance between two consecutive charges on the network chain  $A$  reduces to the Bjerrum length  $Q$  ( $Q = e^2/\epsilon kT$ , where  $e$  is the elementary charge,  $\epsilon$  is the dielectric constant of the solvent,  $k$  and  $T$  are in their usual meaning), counterions start to condense on the network chains. For the present hydrogels swollen in water at  $19^\circ\text{C}$ , the Bjerrum length  $Q$  was calculated as 0.71 nm. The counterion distance  $A$  can also be calculated as  $b/F_2$  where  $b$  is the bond length. Taking  $b = 0.25$  nm (typical value for vinyl polymers) and since  $F_2 = f_2$  (Fig. 3), one obtains the critical value of the AMPS mole fraction in the feed for the onset of counterion condensation as 0.35. Thus, according to the polyelectrolyte theories, if  $f_2 < 0.35$ , all the counterions inside the hydrogels should be free and therefore, they should contribute to the osmotic pressure of the gel [26]. This treatment, however, does not explain the plateau region in Fig. 8 shown between  $f_2 = 0.10$  and 0.20. In fact, ion condensation theories assume rod-like

<sup>1</sup> At high swelling degrees, the effects of entropy and enthalpy of mixing (Eq. (9a)) are negligible compared to the mixing entropy of counterions (Eq. (9c)). Therefore, balancing Eqs. (9b) and (9c) gives the scaling parameter 1.5.



polyelectrolytes in an infinitely diluted solution, which is far from the actual behavior of hydrogels.

In the following paragraphs, the swelling behavior of the hydrogels was analyzed within the framework of the Flory–Rehner theory of swelling equilibrium including the ideal Donnan equilibria. According to the Flory–Rehner theory, the osmotic pressure  $\pi$  of a gel is the sum of three contributions [27,28]:

$$\pi = \pi_{\text{mix}} + \pi_{\text{el}} + \pi_{\text{ion}} \quad (9)$$

where  $\pi_{\text{mix}}$ ,  $\pi_{\text{el}}$ , and  $\pi_{\text{ion}}$  are the osmotic pressures due to polymer–solvent mixing (*mix*), due to deformation of network chains to a more elongated state (*el*), and due to the nonuniform distribution of mobile counterions between the gel and the solution (*ion*), respectively. Osmotic pressure  $\pi$  of a gel determines whether the gel tends to expand or to shrink. When nonzero,  $\pi$  provides a driving force for gel volume change. Solvent moves into or out of the gel until  $\pi$  is zero, i.e. until the forces acting on the gel are balanced.

According to the Flory–Huggins theory,  $\pi_{\text{mix}}$  is given by [15]:

$$\pi_{\text{mix}} = -\frac{RT}{\bar{V}_1} (\ln(1 - v_2) + v_2 + \chi v_2^2) \quad (9a)$$

where  $v_2$  is the volume fraction of polymer in the hydrogel, i.e.  $v_2 = 1/q_v$ ,  $\chi$  is the polymer–solvent interaction parameter,  $\bar{V}_1$  is the molar volume of the solvent (18 ml/g),  $R$  and  $T$  have the usual meaning. To describe the elastic contribution  $\pi_{\text{el}}$ , we will use here the simplest affine network model to describe the behavior of our gels [15]:

$$\pi_{\text{el}} = -\frac{RT}{\bar{V}_1} N^{-1} (v_2^{1/3} v_0^{2/3} - v_2/2) \quad (9b)$$

where  $N$  is the average number of segments in the network chain and  $v_0$  is the volume fraction of the network after synthesis, which is given by Eq. (4). Ionic contribution  $\pi_{\text{ion}}$  to the swelling pressure is caused by the concentration difference of counterions between the gel and the outer solution.

$$\pi_{\text{ion}} = RT \sum_i (C_i^{\text{g}} - C_i^{\text{s}}) \quad (9c)$$

where  $C_i$  is the mobile ion concentration of species  $i$ , the superscripts  $\text{g}$  and  $\text{s}$  denote the gel and solution phases, respectively. The ideal Donnan equilibria for univalent salts like NaCl require the following equality:

$$C_+^{\text{g}} C_-^{\text{g}} = C_+^{\text{s}} C_-^{\text{s}} = C_{\text{salt}}^{\text{s}2} \quad (10)$$

where  $C_{\text{salt}}^{\text{s}}$  represents the salt concentration in the external solution, which was varied between 0 and  $10^{-3}$  mM in our experiments. Moreover, the condition of electroneutrality inside an anionic hydrogel requires:

$$C_+^{\text{g}} = C_-^{\text{g}} + C_{\text{fix}} \quad (11)$$

where  $C_{\text{fix}}$  is the concentration of fixed charges in the gel,

i.e.

$$C_{\text{fix}} = \frac{f}{\bar{V}_r} v_2 \quad (12)$$

where  $f$  is the effective charge density, i.e. the mole fraction of the charged units in the network chains, and  $\bar{V}_r$  is the molar volume of a polymer repeat unit.  $\bar{V}_r$  can be calculated from the mole fraction  $F_2$  of AMPS units in the network as  $\bar{V}_r = 52.6 + 117 F_2$ . Using Eqs. (9)–(12), we obtain the following equation describing the equilibrium swelling degree  $v_2$  of the hydrogels in an aqueous solution of univalent salts:

$$\begin{aligned} \ln(1 - v_2) + v_2 + \chi v_2^2 + N^{-1} (v_2^{1/3} v_0^{2/3} - v_2/2) \\ - \bar{V}_1 \sqrt{\left(\frac{f v_2}{\bar{V}_r}\right)^2 + (2C_{\text{salt}}^{\text{s}})^2} + 2\bar{V}_1 C_{\text{salt}}^{\text{s}} \\ = 0 \end{aligned} \quad (13)$$

The solution of Eq. (13) for the equilibrium volume swelling ratio of the hydrogels  $q_v = 1/v_2$  requires the values of the parameters  $N$ ,  $\chi$ , and  $f$ , characterizing the network and the extent of the network–solvent interactions. In our previous work, we calculated  $N$  as 800 for nonionic AAm-based hydrogels prepared under the same reaction condition as the present hydrogels [14]. Since both the crosslinker ratio and the initial monomer concentrations were fixed in our experiments and, since the polymerization kinetics is independent of the monomer feed composition, it is reasonable to assume a constant crosslink density for all the hydrogels. Thus,  $N = 800$  should be valid for all ionic hydrogels.

The  $\chi$  parameter value for the PAAm–water system was recently evaluated from the swelling data for uncharged PAAm hydrogels swollen in water [29]. A best-fit value for  $\chi$  of 0.48 was obtained [30]. This value of the  $\chi$  parameter provided a good fit to the experimental swelling data of acrylamide-based anionic, cationic, and ampholytic hydrogels of various compositions [30,31]. In the following calculations,  $\chi$  was held constant at this value. It must be pointed out that the  $\chi$  parameter is independent of the number of charges created on the network chains, since this effect is included in Eq. (9c). However, increasing AMPS content in the hydrogels from 0 to 100 mol% changes the chemical structure of the network chains, which may alter the value of the  $\chi$  parameter. In order to take this effect into account, we tried to calculate  $\chi$  from the swelling ratio of the hydrogels in concentrated NaCl solution, where the network chains should behave more like an uncharged polymer. If we assume that at  $C_{\text{salt}}^{\text{s}} = 1$  M, all ionic gels behave as nonionic ones ( $f = 0$ ), Eq. (13) can be applied to the swelling data obtained in 1 M solutions and the  $\chi$  parameter can be calculated. Calculations using the swelling ratio of hydrogels with  $F_2 < 0.40$  gave a constant value for  $\chi$  indicating that  $\chi$  does not change with the AMPS content of the hydrogels. However, the relatively

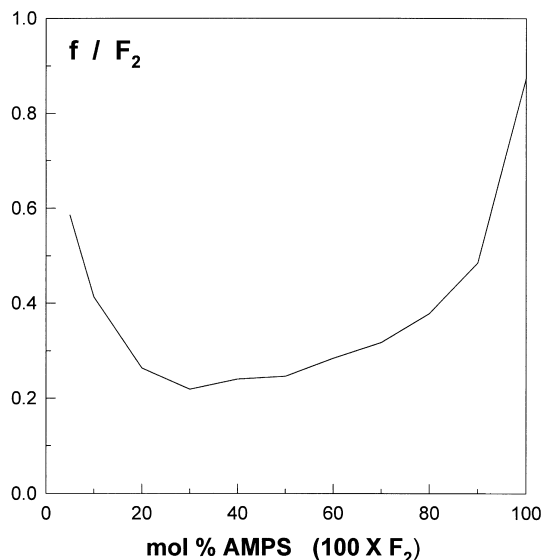


Fig. 10. The fraction of counterions which are effective in gel swelling,  $f/F_2$ , calculated using the Flory–Rehner theory, shown as a function of the AMPS content of the hydrogels.

high and  $C_{\text{salt}}^{\text{s}}$  dependent swelling behavior of hydrogels with  $F_2 > 0.40$  did not allow the calculation of  $\chi$  in salt solution. This behavior indicates that the expansion of the network chains due to charged groups cannot be totally screened even in 1 M NaCl solution. This is in fact in accord with the results observed for linear AMPS based polymers [7].

In order to solve Eq. (13) for  $q_v$ , the fraction of charged units in the network chains,  $f$ , must also be known. Assuming  $f = F_2$ , swelling calculations led to poor agreement between theory and experiment. Therefore, we calculated the  $f$  value of the ionic hydrogels from their equilibrium swelling ratio in water and using Eq. (13) for the condition  $C_{\text{salt}}^{\text{s}} = 0$ . The calculation results are collected in Fig. 10 as the dependence of the fraction of counterions which are effective in gel swelling ( $f/F_2$ ) plotted as a function of the AMPS content of the hydrogels. It is seen that, at 5 mol% AMPS content, only about 60% of the counterions contribute to the gel swelling whereas this value decreases as the AMPS content increases and becomes nearly constant between 20 and 60 mol% AMPS. Thereafter, it increases again with increasing AMPS content.

Fig. 10 indicates that, according to the Flory–Rehner theory, all the counterions inside the gel are not effective in the gel swelling. Recent experimental and theoretical results also indicate the existence of “osmotically passive” counterions inside the swollen gel which do not contribute to the swelling process [10,30,32]. A possible explanation is the hydrophobic interactions between the alkyl groups of the AMPS units leading to the formation of aggregates; the counterions in these aggregates may condense and lead to a decrease in the osmotic pressure. Gel heterogeneities may also be responsible for this phenomena. As we reported in the previous section, the AAm/AMPS copolymerization

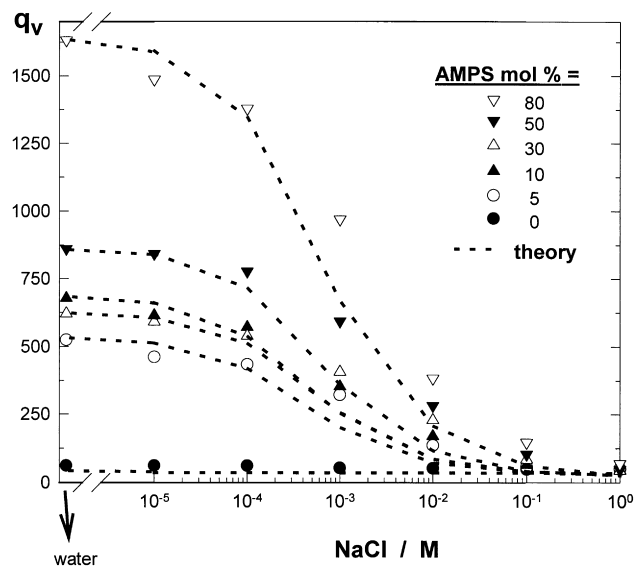


Fig. 11. Comparison of the predictions of the Flory–Rehner theory of swelling equilibrium with the experimental swelling data of the hydrogels in aqueous NaCl solutions.

system became heterogeneous at the gel point and the gel growth occurred in this heterogeneous system. The gel formed in such a system should exhibit nonuniform distribution of crosslinks [6]. The counterions in the highly cross-linked (less swollen) regions of the gel may condense on the network chains and become passive in the gel swelling.

Using the parameter  $f$  calculated from the swelling ratio of the hydrogels in water, we can now predict using Eq. (13) the equilibrium swelling ratio  $q_v$  of the hydrogels in aqueous NaCl solutions. Some of the calculation results are shown in Fig. 11 as the dotted curves. It is seen that the prediction of Eq. (13) for  $q_v$  is good; some deviations appear between  $10^{-4}$  and  $10^{-2}$  M, where the gel deswells more smoothly than predicted by the theory. We can conclude that the Flory–Rehner theory correctly predicts the swelling behavior of the hydrogels if their charge densities are taken as an adjustable parameter. The effective charge density  $f$  thus evaluated is much lower than the nominal charge density  $F_2$ .

Another approach to interpret the equilibrium swelling data of the hydrogels is to use their effective excluded volume as the independent variable [33]. The effective excluded volume is controlled by the parameter  $f/\kappa$ , where  $\kappa$  is the inverse of the Debye–Huckel radius, i.e.

$$\kappa^2 = 4\pi Q(C_+^{\text{g}} + C_-^{\text{g}}) \quad (14)$$

It was shown that  $f/\kappa$  determines the extent of gel swelling both in dilute and concentrated salt solutions and scales with  $q_v$  as  $q_v \propto (f/\kappa)^{1.2}$  [33].

By the substitution of Eqs. (10)–(12) into Eq. (14), the following equation was obtained for the Debye–Huckel radius of the present hydrogels:

$$\kappa^2 = 4\pi Q \sqrt{\left(\frac{fv_2}{V_r}\right)^2 + (2C_{\text{salt}}^{\text{s}})^2} \quad (14a)$$

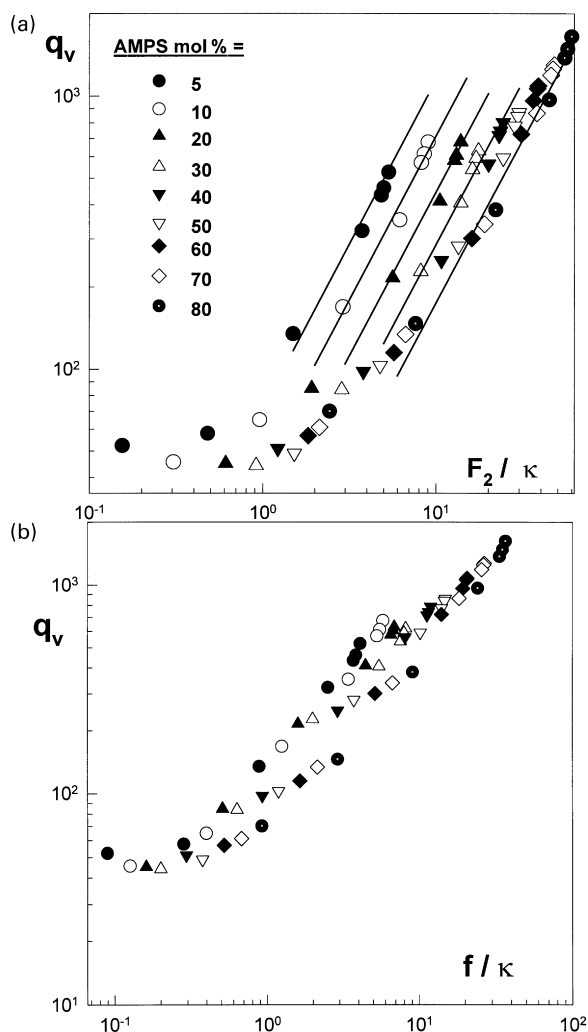


Fig. 12. The variation of the equilibrium volume swelling ratio of the hydrogels  $q_v$  in water and in NaCl solutions of concentrations ranging from  $10^{-5}$  to 1 M with the effective excluded volume parameter (a)  $F_2/\kappa$  and (b)  $f/\kappa$ . The solid lines in (a) show the theoretical slope 1.2.

In Fig. 12a and b, all the equilibrium volume swelling data of the hydrogels in water and in NaCl solutions are collected and shown in a double logarithmic scale as functions of  $F_2/\kappa$  and  $f/\kappa$  respectively. The solid lines in Fig. 12a illustrate the theoretical slope of 1.2. It is seen that, if the nominal charge density of the hydrogels  $F_2$  is used in the calculations (Fig. 12a), the slope of  $\log(q_v)$  versus  $\log(F_2/\kappa)$  plots for swelling ratios larger than  $10^2$  is close to the theoretical value of 1.2. Deviations appear at swelling ratios smaller than  $10^2$  and the slope approaches to zero at  $F_2/\kappa < 1$  due to the screening of the charges on the network chains. On the contrary, using the charge density  $f$  found by the Flory–Rehner theory, one obtains the  $q_v$  versus  $f/\kappa$  plot shown in Fig. 12b. Here, the slope of the double logarithmic plot is close to zero at high salt concentrations and it increases as  $f/\kappa$  increases and approaches 1.8 in dilute salt solutions. Although a theory is needed to explain the relations shown in Fig. 12a and b,  $F_2/\kappa$  and  $f/\kappa$  are seen to be powerful independent variables

to represent the swelling data of the hydrogels in a single graph.

#### 4. Conclusions

In this work, the relation between the formation mechanism and the swelling behavior of AAm/AMPS-based hydrogels was studied. The hydrogels were prepared by free-radical crosslinking copolymerization of AAm and AMPS at  $40^\circ\text{C}$  in the presence of BAAM as the crosslinker. Both the crosslinker ratio and the initial monomer concentration were fixed at 1/82 and 0.700 M, respectively, while the AMPS content in the monomer mixture was varied from 0 to 100 mol%. By i.r. and e.m. techniques, it was shown that the copolymer composition is equal to the monomer feed composition. The monomer conversion versus time histories as well as the growth rate of the gel during the reactions were found to be independent of the amount of AMPS in the initial monomer mixture. It was shown that the reaction system separates into two phases at the gel point and the gel growth takes place in a heterogeneous system. The equilibrium degree of swelling of the final hydrogels increases with increasing ionic group content of the hydrogels until a plateau is reached at about 10 mol% AMPS. Between 10 and 30 mol% AMPS, the equilibrium gel swelling in water as well as in aqueous NaCl solutions was independent of the ionic group content of the hydrogels. Further increase in the AMPS content beyond this value increased the gel swelling continuously up to 100 mol%. The polyelectrolyte theories based on the counterion condensation cannot explain the observed swelling behavior of AAm/AMPS hydrogels. Using the Flory–Rehner theory of swelling equilibrium including the ideal Donnan equilibria, it was shown that the existence of counterions inside the hydrogel which are ineffective in the gel swelling is responsible for the observed swelling behavior.

#### Acknowledgements

Work was supported by the Scientific and Technical Research Council of Turkey (TUBITAK), TBAG-1561 and by the Istanbul Technical University Research Fund, ITU-1054.

#### References

- [1] Tanaka T. Phys Rev Lett 1978;40:820.
- [2] Shibayama M, Tanaka T. Adv Polym Sci 1993;109:1.
- [3] Baselga J, Llorente MA, Hernandez-Fuendez I, Pierolo IF. Eur Polym J 1989;25:471.
- [4] Tobita H, Hamielec AE. Polymer 1990;31:1546.
- [5] Naghash HJ, Okay O. J Appl Polym Sci 1996;60:971.
- [6] Funke W, Okay O, Joos-Muller B. Adv Polym Sci 1998;136:139.
- [7] Fisher LW, Sochor AR, Tan JS. Macromolecules 1977;10:949.
- [8] Liu X, Tong Z, Hu O. Macromolecules 1995;28:3813.
- [9] Tong Z, Liu X. Macromolecules 1994;27:844.

- [10] Okay O, Sariisik SB, Zor SD. *J Appl Polym Sci* 1998;70:567.
- [11] Ilavsky M. *Macromolecules* 1982;15:782.
- [12] Gooda SR, Huglin MB. *Macromolecules* 1992;25:4215.
- [13] Stewart JE. *Infrared spectroscopy, experimental methods and techniques*, New York: Marcel Dekker, 1970. p. 524.
- [14] Durmaz S, Okay O. In preparation.
- [15] Flory PJ. *Principles of polymer chemistry*, Ithaca, New York: Cornell University Press, 1953.
- [16] Okay O. *Polymer* 1994;35:2613.
- [17] Tobita H. *Macromolecules* 1993;26:5427.
- [18] Zhu S, Ma M, Zhou W. *Macromolecules* 1996;29:5688.
- [19] Beranova H, Dusek K. *Collection Czech Chem Comm* 1969;34:2932.
- [20] Silberberg-Bouhnik M, Ramon O, Ladyzhinski I, Mizrahi S. *J Polym Sci Polym Phys* 1995;33:2269.
- [21] Bromberg L, Grosberg AY, Matsuo ES, Suzuki Y, Tanaka T. *J Chem Phys* 1997;106:2906.
- [22] Tong Z, Liu X. *Eur Polym J* 1993;29:705.
- [23] Konak C, Bansil R. *Polymer* 1989;30:677.
- [24] Hasa J, Ilavsky M, Dusek K. *J Polym Sci Phys Ed* 1975;13:253.
- [25] Manning GS. *J Chem Phys* 1969;51:924.
- [26] Schroder UP, Opperman W. *Properties of polyelectrolyte gels*. In: Cohen-Addad JP, editor. *Physical properties of polymeric gels*, New York: Wiley, 1996. p. 19.
- [27] Flory PJ, Rehner Jr J. *J Chem Phys* 1943;11:521.
- [28] Frenkel J. *Rubber Chem Technol* 1940;13:264.
- [29] Hooper HH, Baker JP, Blanch HW, Prausnitz JM. *Macromolecules* 1990;23:1096.
- [30] Baker JP, Hong LH, Blanch HW, Prausnitz JM. *Macromolecules* 1994;27:1446.
- [31] Baker JP, Blanch HW, Prausnitz JM. *Polymer* 1995;36:1061.
- [32] Philippova OE, Rulkens R, Koutunenko BI, Abramchuk SS, Khokhlov AR, Wegner G. *Macromolecules* 1998;31:1168.
- [33] Skouri R, Schosseler F, Munch JP, Candau SJ. *Macromolecules* 1995;28:197.